EURASIAN JOURNAL OF MATHEMATICAL AND COMPUTER APPLICATIONS
ISSN 2306–6172
Volume 12, Issue 4 (2024) 140 – 149

NUMERICAL STUDY OF JET FLOW CONTROL USING ACOUSTIC PERTURBATIONS

Vankova O.S., Yakovenko S.N.

Abstract The article presents the results of a numerical study of flow control in a submerged round jet using harmonic perturbations at the lateral boundaries simulating sound sources. The analysis of distributions of instantaneous and time-averaged components of the velocity vector is performed, and physical effects occurring in the excited jet are revealed. At certain values of the Strouhal and Reynolds numbers, a bifurcation occurs in the jet caused by acoustic excitation, as in other studies with mechanical forcing or disturbances of the inlet velocity profile. The effect of the transition from one to two loudspeakers located on opposite boundaries on the mean velocity field and the jet flow structure is studied.

Key words: round jet, harmonic perturbation, sound sources, flow bifurcation, numerical simulation, flow control.

AMS Mathematics Subject Classification: 76-10, 76D05, 76D25, 76D55, 76M12.

DOI: 10.32523/2306-6172-2024-12-4-140-149

1 Introduction

Jet flow control methods are needed in many technical applications to solve problems of reducing the temperature of heated surfaces, noise in jets, fuel consumption, and the emission of harmful impurities. At relatively low excitation frequencies, the entrainment of fluid particles from the external environment and mixing in the jet increases [1, 2], leading to heat and mass transfer intensification. Acoustic or mechanical forcing on the flow region near the nozzle increases the expansion of the jet, causing its meandering and splitting. In previous works [2–14], the main results of visualization, measurements, and numerical simulations on the branching of burning and cold jets under excitations in various ways for laminar and turbulent outflow from orifices of various shapes have been presented.

One of the methods of active flow control in a jet widely used in physical experiments is the transverse acoustic field forcing from one, two or more sound sources. However, in computational experiments, such a method of flow disturbance has almost never been used, in contrast to the disturbance of the inlet velocity profile [10, 11, 12] or transverse vibrations of the inlet boundary [13, 14]. We can only note the simulation results [15] in a round jet with a sound source located on the lateral boundary, as in the physical experiments [4–9].

In the present paper, the results of calculations of a free round jet excited by a transverse acoustic field from two sound sources on opposite transverse boundaries are presented for the first time, in comparison to those with a single source. The

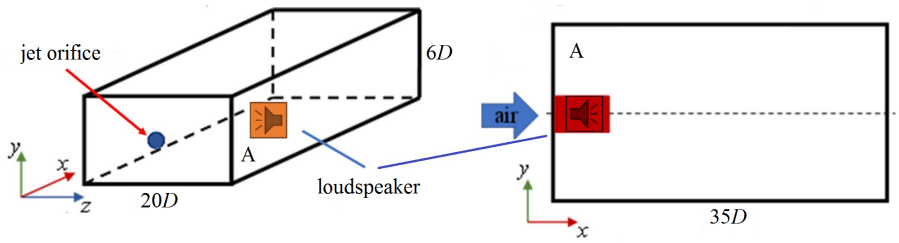

Figure 1: Scheme of the computation domain for a round jet with transverse acoustic forcing from a single loudspeaker: three-dimensional view (left), side view (right).

issues of grid convergence and obtaining a solution independent of other parameters of the computational algorithm, such as the domain size, the time of relaxation to a quasi-steady flow pattern, and the averaging period are also discussed.

2 Mathematical problem set-up

To predict a jet flow, three-dimensional unsteady Navier–Stokes equations are used in the incompressible fluid approximation:

$$\frac{\partial u_i}{\partial x_i} = 0, \quad \frac{\partial u_i}{\partial t} + u_j \frac{\partial u_i}{\partial x_j} = -\frac{1}{\rho}\frac{\partial p}{\partial x_i} + \nu \frac{\partial^2 u_i}{\partial x_j^2}$$

where $u_i = (u, v, w)$ are the velocity vector components, p is pressure, t is time, $x_i = (x, y, z)$ are spatial coordinates in the axial direction (x) of a jet outflow and lateral directions (y, z). Values of density ρ and kinematic viscosity ν are assumed to be constant in the jet flow domain.

The initial conditions inside the rectangular region (Figure 1) for the above system of equations, which determines the dependence of four physical quantities on independent variables (x, y, z, t), correspond to a fluid at rest ($u = v = w = 0$, $p = 1$ atm), with the exception of the boundary through which the jet flows into the computational domain, and the sections of the lateral boundaries where disturbances are introduced.

At the inlet boundary ($x = 0$), no-slip conditions are specified for the velocity components ($u = v = w = 0$), with the exception of the orifice in the inlet boundary through which the jet flows into the domain. When modeling a round air jet flowing out at constant velocity U into a submerged space from an orifice of diameter D centered at the $x = y = z = 0$ point, we have $u(x = 0) = U$ for $r < R$, $u(x = 0) = 0$ for $r \geq R$ (where $R = D/2$ is the orifice radius). The Reynolds number $\mathrm{Re} = UD/\nu$ is chosen to be 500, which for an air jet with $D = 1$ mm gives $U \approx 8$ m/s, i.e. much less than the sound speed. The choice of a relatively small value of Re is due, firstly, to acceptable grid convergence (see below) on the available computing resources, while at $\mathrm{Re} > 500$ grid convergence in the direct numerical solution of the Navier–Stokes equations is not achieved in the considered computation domain. Secondly, there are data for $\mathrm{Re} = 500$ from previous calculations [13–16] with transverse disturbances in various ways, which can be used for comparison with the obtained results. Thirdly, laminar jets in physical experiments with a transverse acoustic field had Reynolds numbers from 20 to 4000

[5–9], and the Re value considered in the work falls approximately in the center of this range.

As an acoustic forcing on the face A (Figure 1), source 1 is specified, with a harmonic oscillation of the transverse velocity $w(t) = a \times sin(2\pi ft)$, where $a = 0.1U$ is the disturbance amplitude, f is its frequency at the Strouhal number $\mathrm{St} = fD/U$, specified as $\mathrm{St} = 0.1$. Source 1 with the center at the point $x/D = 2.5, y/D = 0, z/D = 10$ is localized in a rectangular area of $5D \times 6D$, i.e. it occupies the part of the lateral boundary adjacent to the inlet section. For the case of two speakers, source 2 occupies the part of the opposite lateral boundary adjacent to the inlet section in the area of $5D \times 6D$ with the center at $x/D = 2.5, y/D = 0, z/D = -10$.

On the remaining parts of the lateral faces of the domain (where there are no sources of oscillations) and on the outlet boundary ($x \longrightarrow \infty$), mild conditions are set (zero velocity gradients along the normal to the boundary). Zero pressure gradients along the normal to all boundaries are also set. This statement is due to the fact that detailed information on instantaneous values of velocity and pressure is absent in physical experiments. It is also possible to set more rigid conditions, in particular, zero velocity and constant (atmospheric) pressure on the lateral boundaries. If lateral boundaries are located far enough from the jet periphery (where the velocity is equal to 5-10% of its maximum in this section), and the outlet boundary is far from the point of the splitting start, where the transformation of the vortex structure of a flow occurs, then the incorrectness of boundary conditions will not noticeably affect results obtained.

3 Numerical realization

The numerical solution of the Navier–Stokes equations (using direct numerical simulation, where turbulence models are not introduced) for a flow including a free jet and sound sources is performed by means of the ANSYS Fluent package using the finite volume method, in which the computation domain is divided into a set of computational cells. The PISO method is used to determine the velocity and pressure fields, based on the "predictor-corrector" approach, which is suitable for the numerical study of unsteady flows.

Oscillations are introduced with a user-defined function implemented in the calculation algorithm: the "velocity-inlet" boundary condition is selected, where the velocity of an inflow entering through the boundary with the direction normal to the boundary is specified. The "pressure-outlet" conditions on other boundaries (except for the jet inlet and sound sources) allow the flow to exit or enter the computation domain.

The domain dimensions ($35D \times 6D \times 20D$), time step $\Delta t = 0.05D/U$ and the number of non-uniform mesh cells in the $x-y-z$ directions were chosen taking into account the problem statement in previous numerical studies [9–14]. At the same time, the optimal mesh resolution turned out to be coarser for the considered case of a sufficiently small Reynolds number. In particular, to save computational resources, the minimum cell sizes of the optimal mesh near the jet inlet were taken to be about $D/16$, which is sufficient to identify the effects of jet bifurcation and obtain mesh convergence (see below). Studies of the convergence of the solution with refinement of the coordinate

Mesh	Cell size	Total cell number	Cells at $r \leq 0.5D$	q_{x1}	q_{x2}	q_y	q_z
1	$D/12$	552 080	108	1.0132	1.066	1.132	1.066
2	$D/16$	1 325 032	192	1.0100	1.050	1.100	1.050
3	$D/21$	3 127 236	341	1.0076	1.038	1.076	1.038

Table 1: Parameters of coarse, optimal, and fine computational meshes 1–3.

and time steps show that further reduction of the spatial or time step and increase in the domain do not lead to visible changes.

The solution was studied for independence from numerical parameters in calculations on successive meshes. Three meshes with minimum cell sizes $D/12$, $D/16$ and $D/21$ were considered, consisting of several blocks: a uniform mesh located in the region near the jet entrance at $x \leq 5D$, $|y| \leq 0.75D$, $|z| \leq 0.75D$; blocks with a smoother stretching of the cell size (with coefficient q_{x1}) along the x axis at $5D \leq x \leq 20D$; blocks with a sharper stretching of the cell sizes (with coefficients q_{x2}, q_y, q_z) in all directions at $x \geq 20D$, $|y| \geq 0.75D$, $|z| \geq 0.75D$. The specified division of the mesh into blocks in a number of preliminary test runs is adapted to the features of a flow under study, in which, under the action of transverse perturbations, a transformation of vortex structures occurs, leading to branching of the jet, which are localized near the $y = z = 0$ axis at $x < 20D$ (the issues of vortex interaction are covered in more detail, for example, in [2, 12, 13]). An adequate description of this transformation requires fairly fine grids, which is associated with the presence of sub-regions with uniform or smoothly increasing cells in the central part of the domain at $x < 20D$.

Table 1 presents the parameters of the considered meshes, where q_{x1}, q_{x2}, q_y, q_z are the coefficients of geometric progressions (ratios of linear dimensions of adjacent cells), along which the grids are stretched. When constructing a sequence of grids, all cells of a finer grid differ from a coarser one by the ratios $r_{12} > r_{23} > 1.3$ in accordance with the recommendations of [17].

4 Results

In the first series of numerical studies, the results of calculations on successive meshes 1–3 were compared for the case of two speakers located on opposite lateral boundaries in order to check the possibility of convergence of the solution to a grid-independent velocity field for the given parameters of the problem.

Figure 2 shows the distributions of the velocity averaged over a large time interval, obtained in calculations on different meshes. The typical thickness $d(x) = 0.5(d_1 + d_2)$ and the bifurcation angle α of the jet are evaluated from the curves of the quantities $d_1(x) = |z(\langle u \rangle = \langle u \rangle_{1max})|$ and $d_2(x) = |z(\langle u \rangle = \langle u \rangle_{2max})|$, defined as the absolute values of the coordinate z, where the time-averaged velocity $\langle u \rangle$ within the upper and lower branches of the jet reaches its maximum values. The optimal values ($T_0 = 2T = 1000D/U$) of the time of relaxation of a quasi-steady flow pattern T_0 and the averaging period T over time at $T_0 \leq t \leq T_0 + T$ were determined in separate series

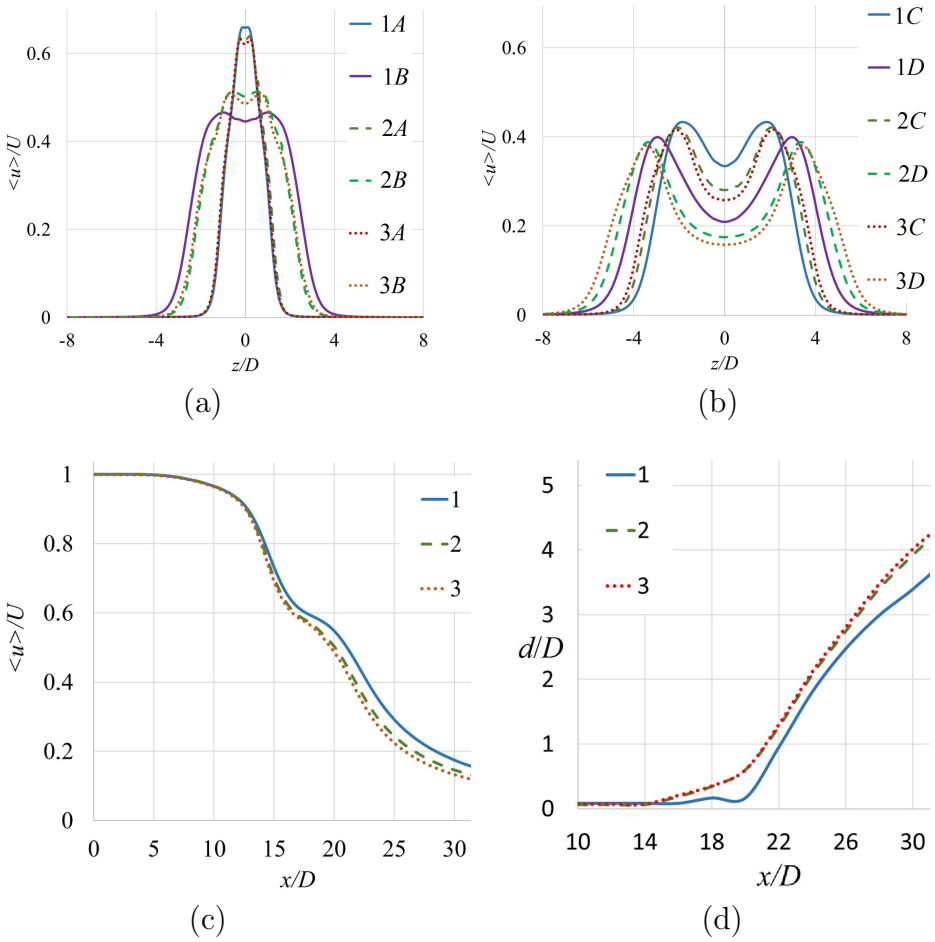

Figure 2: Results of calculations with meshes 1, 2, 3 (lines 1, 2, 3, respectively): time-averaged distributions of the axial velocity vector component $\langle u \rangle$ at different sections $x/D = 16$ (A), 20 (B), 24 (C), 28 (D) of the bifurcation plane $y = 0$ (a, b); on the axis $y = z = 0$ (c); dependence of the typical thickness d on the coordinate x (d).

of successive runs for $T_0U/D = 500$, 750, 1000, 1500, ... (at fixed $T = 500D/U$) and for $TU/D = 250$, 500, 750, 1000, ... (at fixed $T_0 = 1000D/U$) from the condition of a small difference in the distributions of the mean velocity with further increase in the parameters T_0 and T. It is evident from Figure 2 that the results on meshes 2 and 3 with the minimum cell sizes $D/16$ and $D/21$ are close, therefore mesh 2 is considered optimal, and the data obtained with it are used hereafter to analyze the jet behavior with an external forcing.

Figure 3 presents the instantaneous velocity snapshots at different times at $\mathrm{St} = a/U = 0.1$. It is clear how the jet splitting process occurs under the influence of acoustic disturbance: first, its meandering is observed, then at $tU/D \sim 100$, the formation of two branches begins, which ends at $tU/D \sim 1000$, after which, at $1000 \leq tU/D \leq 1500$, averaging is performed.

Figure 4 shows the velocity distributions at other planes (x, y) and (y, z), from which it is evident that the jet bifurcation occurs at $14 < x/D < 18$, and the choice of a narrow region with a width of $6D$ along y for the parameters under consideration is

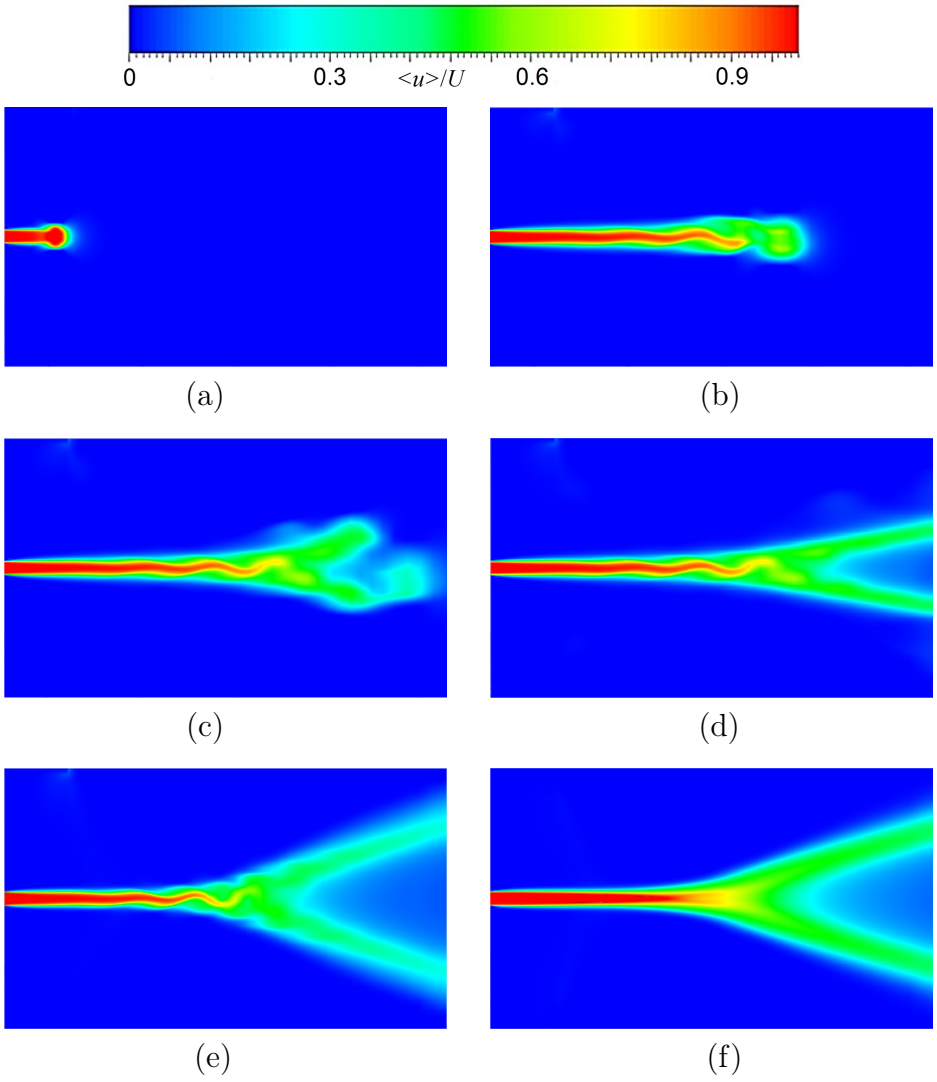

Figure 3: Contours of the axial velocity vector component $u(x, z)$ at the bifurcation plane $y = 0$ for different times $tU/D = 20$ (a), 60 (b), 100 (c), 200 (d), 600 (e), and the velocity $\langle u \rangle(x, z)$, averaged at $1000 \leq tU/D \leq 1500$ (f).

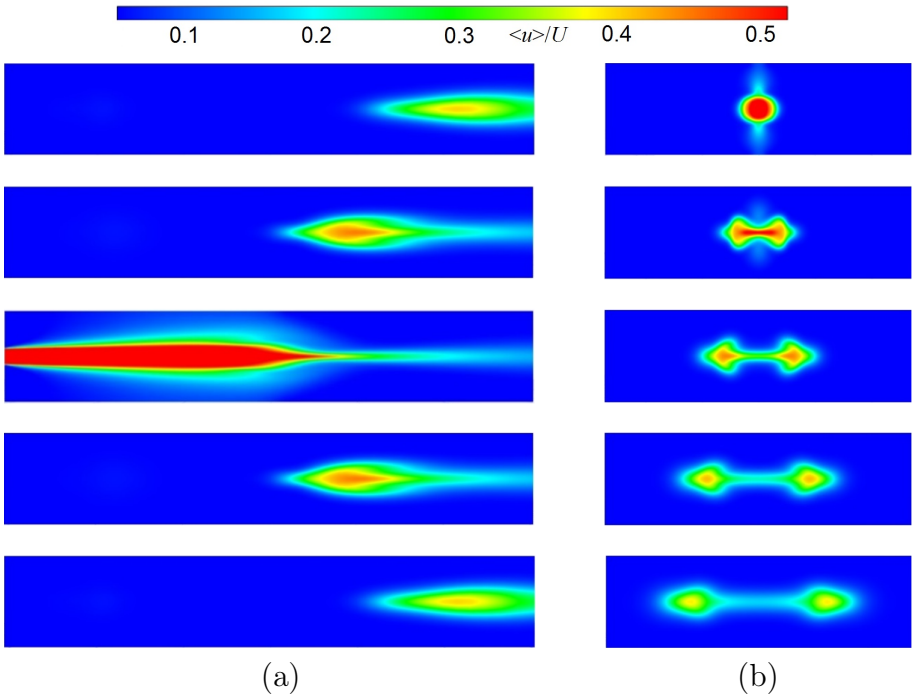

Figure 4: Mean velocity contours at different planes (from top to bottom):
(a) $\langle u \rangle(x, y)$ at $z/D = -4$, -2, 0, 2, 4; (b) $\langle u \rangle(y, z)$ at $x/D = 14$, 18, 22, 26, 30.

justified by the weak expansion of the jet in this direction, in contrast to the z axis, where the width of the domain is taken to be equal to $20D$.

Figure 5 demonstrates the time-averaged velocity distributions for the case of one and two speakers. It is evident that for one speaker the splitting pattern is asymmetric, the splitting branch at $z < 0$ is weaker and shifted away from the point of acoustic perturbation origin, the maximum velocity in it is lower by an average of 8%. At the same time, the amplitudes w_0 of the transverse velocity oscillations on the jet axis $w(y = z = 0) = w_0 \sin(2\pi f t)$ (which cause the flow meandering at some distance downstream from the inlet) for the case of one speaker are approximately two times lower than when two speakers are included, nevertheless the bifurcation angle remains almost unchanged (Figure 5, Table 2).

A qualitative comparison of the obtained results with the visualization data in physical experiments [2-9] shows a similar nature of a flow in the jet with transverse perturbations, in particular, the jet meandering under the influence of an external forcing, then the jet splitting, the starting point and angle of which depend significantly on the frequency, amplitude and type of forcing. In addition, the effect of flattening of a round jet in the lateral plane (x, y) under the action of a transverse acoustic field, noted in the experiments [5-7] and noticeable at $x < 15D$ on the velocity contours (Figure 4), is confirmed.

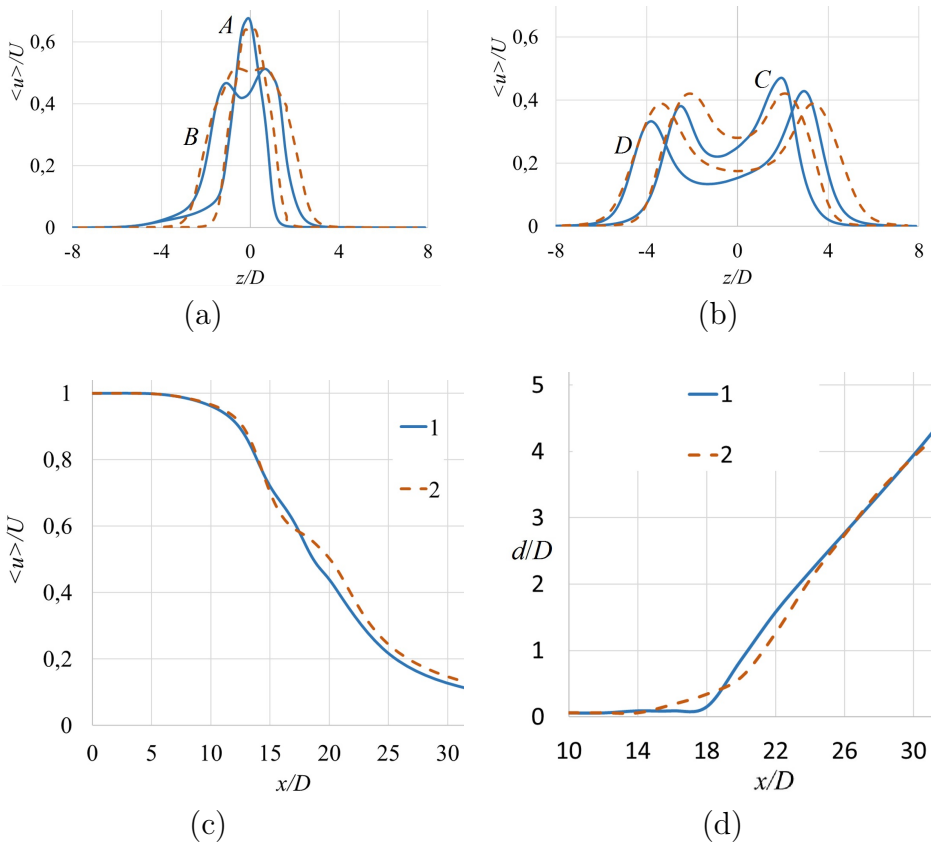

Figure 5: Results of calculations with one (lines 1) and two (lines 2) speakers: time-averaged distributions of the axial velocity vector component $\langle u \rangle$ at different sections $x/D = 16$ (A), 20 (B), 24 (C), 28 (D) of the bifurcation plane $y = 0$ (a, b); on the axis $y = z = 0$ (c); dependence of the typical thickness d on the coordinate x (d).

Table 2: The amplitude w_0 of transverse velocity oscillations at three points on the jet axis and the bifurcation angle α for two cases with one and two speakers.

Cases of simulation	$\frac{w_0(x=2.5D)}{U}$	$\frac{w_0(x=5.0D)}{U}$	$\frac{w_0(x=7.5D)}{U}$	α
one speaker	0.17%	0.37%	1.04%	45.91°
two speakers	0.33%	0.70%	1.91%	41.18°

5 Conclusion

The paper analyzes the results of numerical simulation of a free round jet with transverse excitation using single-mode acoustic forcing from one or two sound sources located on the lateral boundary or on opposite lateral boundaries. It should be noted that the numerical study of jet bifurcation under the influence of two sources was performed for the first time. Comparison of these results with those of previous works [13-15] in the presence of vibration excitation shows an identical flow pattern for the considered sufficiently weak perturbation amplitudes. For future research, it is of interest to study jets with external forcing in wide ranges of Re, St numbers, forcing amplitudes, density drops, for different nozzle shapes, and a greater (than two) number of disturbance sources.

Acknowledgement

The study has been supported by a grant No. 23-27-00310 of Russian Science Foundation, `https://rscf.ru/en/project/23-27-00310/`.

References

[1] Ginevsky A.S., Vlasov Ye.V., Karavosov R.K., *Acoustic control of turbulent jets*, Springer, Berlin, 2004.

[2] Reynolds W.C., Parekh D.E., Juvet P.J.D., Lee M.J.D., *Bifurcating and blooming jets*, Annu. Rev. Fluid Mech., Vol. 35 (2003), 295–315.

[3] Parekh D.E., Reynolds W.C., Mungal M.G., *Bifurcation of round air jets by dual-mode acoustic excitation*, AIAA Paper 87-0164 (1987).

[4] Suzuki M., Atarashi T., Masuda W., *Behavior and structure of internal fuel-jet in diffusion flame under transverse acoustic excitation*, Combust. Sci. Tech., Vol. 179 (2007), 2581–2597.

[5] Kozlov V.V., Grek G.R., Litvinenko Yu.A., *Visualization of conventional and combusting subsonic jet instabilities*, Springer International Publishing, Dordrecht, 2016.

[6] Kozlov V.V., Grek G.R., Litvinenko Yu.A., Kozlov G.V., Litvinenko M.V., *Subsonic round and plane macro- and microjets in a transverse acoustic field*, Vestn. NGU. Ser. Fiz., Vol. 5, Iss. 2 (2010), 28–42. (in Russian)

[7] Kozlov V.V., Grek G.R., Korobeynichev O.P., Litvinenko Yu.A., Shmakov A.G., *Features of hydrogen combustion in a round and flat jet in a transverse acoustic field and their comparison with the results of propane combustion under the same conditions*, Vestn. NGU. Ser. Fiz., Vol. 9, Iss. 1 (2014), 79–86. (in Russian)

[8] Krivokorytov M.S., Golub V.V., Volodin V.V., *The effect of acoustic oscillations on diffusion combustion of methane*, Tech. Phys. Lett., Vol. 38 (2012), 478–480.

[9] Krivokorytov M.S., Golub V.V., Moralev I.A., *The evolution of instabilities in gas microjets under acoustic action*, Tech. Phys. Lett., Vol. 39 (2013), 814–817.

[10] Tyliszczak A., *Multi-armed jets: a subset of the blooming jets*, Phys. Fluids, Vol. 27 (2015), 041703.

[11] Tyliszczak A., *Parametric study of multi-armed jets*, Int. J. Heat Fluid Flow, Vol. 73 (2018), 82–102.

[12] Gohil T.B., Saha A.K., *Numerical simulation of forced circular jets: effect of flapping perturbation*, Phys. Fluids, Vol. 31 (2019), 083602.

[13] Shevchenko A.K., Yakovenko S.N., *Numerical study of flow control methods and splitting effects in a round submerged jet*, Thermophysics and Aeromechanics, Vol. 28 (2021), 353–368.

[14] Shevchenko A.K., Yakovenko S.N., *Active ways of flow and mass-transfer control in round jets with and without impingement*, AIP Conf. Proc., Vol. 2504 (2023), 030050.

[15] Vankova O.S., Yakovenko S.N., *Numerical simulations of a subsonic round jet with transverse acoustic and mechanical forcing*, E3S Web Conf., Vol. 459 (2023), 03002.

[16] Koumoutsakos P., Freund J., Parekh D., *Evolution strategies for automatic optimization of the jet mixing*, AIAA J., Vol. 39 (2001), 967–969.

[17] Celik I., Ghia G., Roache P.J., Freitas C.J., Coleman H., Raad P.E., *Active ways of flow and mass-transfer control in round jets with and without impingement*, Procedure for estimation and reporting of uncertainty due to discretization in CFD applications, Vol. 130 (2008), 078001.

Olga S. Vankova,
Khristianovich Institute of Theoretical and Applied Mechanics, SB RAS,
Russia, 630090, Novosibirsk, Institutskaya Str., 4/1
Email: vankova@itam.nsc.ru

Sergey N. Yakovenko,
Khristianovich Institute of Theoretical and Applied Mechanics, SB RAS,
Russia, 630090, Novosibirsk, Institutskaya Str., 4/1
Email: yakovenk@itam.nsc.ru

Received 13.08.2024, Accepted 07.10.2024